SPORTS BIOMECHANICS
https://doi.org/10.1080/14763141.2022.2164345

Routledge
Taylor & Francis Group

Peak tibial acceleration should not be used as indicator of tibial bone loading during running

Marit A. Zandbergen[a,b], Xanthe J. Ter Wengel[a], Robbert P. van Middelaar[a], Jaap H. Buurke[a,b], Peter H. Veltink[a] and Jasper Reenalda[a,b]

[a]Department of Biomedical Signals and Systems, Faculty of Electrical Engineering, Mathematics and Computer Science (EEMCS), University of Twente, Enschede, The Netherlands; [b]Department of Rehabilitation Technology, Roessingh Research and Development, Enschede, The Netherlands

ABSTRACT

Peak tibial acceleration (PTA) is a widely used indicator of tibial bone loading. Indirect bone loading measures are of interest to reduce the risk of stress fractures during running. However, tibial compressive forces are caused by both internal muscle forces and external ground reaction forces. PTA might reflect forces from outside the body, but likely not the compressive force from muscles on the tibial bone. Hence, the strength of the relationship between PTA and maximum tibial compression forces in rearfoot-striking runners was investigated. Twelve runners ran on an instrumented treadmill while tibial acceleration was captured with accelerometers. Force plate and inertial measurement unit data were spatially aligned with a novel method based on the centre of pressure crossing a virtual toe marker. The correlation coefficient between maximum tibial compression forces and PTA was 0.04 ± 0.14 with a range of −0.15 to +0.28. This study showed a very weak and non-significant correlation between PTA and maximum tibial compression forces while running on a level treadmill at a single speed. Hence, PTA as an indicator for tibial bone loading should be reconsidered, as PTA does not provide a complete picture of both internal and external compressive forces on the tibial bone.

ARTICLE HISTORY
Received 7 June 2022
Accepted 27 December 2022

KEYWORDS
Accelerometer; bone stress injury; compression forces; inertial measurement unit; injury risk; running biomechanics

Introduction

Runners are at high risk of developing bone stress fractures. Stress fractures account for 3% to 14% of running injuries (James et al., 1978; McBryde, 1985; Taunton et al., 2002) and are most prevalent in the distal part of the tibial bone (20% to 53%) (Romani et al., 2002; Wall & Feller, 2006). Stress fractures are the result of prolonged and repetitive forces on the bone without enough rest for bone remodelling (Harrast & Colonno, 2010; Umans & Pavlov, 1994). Stress fracture risk is influenced by both fixed factors, such as sex, skeleton alignment, bone geometry, bone remodelling, and bone mineral density, and variable factors, such as training intensity, training frequency, training surface, footwear, running incline, and running kinematics (Edwards, 2018; Harrast & Colonno, 2010; Pohl et al., 2008; Saunier & Chapurlat, 2018; Umans & Pavlov, 1994). Forces on the tibia and subsequent tibial bone deformation can only

CONTACT Marit A. Zandbergen m.a.zandbergen@utwente.nl

be directly measured in vivo after an invasive surgery (Komi, 1990; Lanyon et al., 1975; Milgrom et al., 2000). Hence, there is a lot of interest in indirect measures of tibial bone forces.

Ground reaction forces (GRFs) and peak tibial accelerations (PTAs) are often used as surrogate measures for tibial bone loading and injury risk in running (Bigelow et al., 2013; Chadefaux et al., 2019; García-Pérez et al., 2014; Lafortune et al., 1996; Lucas-Cuevas et al., 2015; Milner et al., 2006; Mizrahi et al., 2000; Zadpoor & Nikooyan, 2011). GRF is the force exerted by the ground on the body to support the body weight (BW) and, in addition, results in acceleration and deceleration of the body's centre of mass during the stance phase of running. The collision of the foot with the ground causes an impact shock that travels through the body (Lafortune et al., 1996). PTA reflects this impact shock at the surface of the skin near the tibia bone (Sheerin et al., 2019). PTA occurs shortly after initial contact and negligibly to moderately correlates with the slope of the vertical GRF and GRF impact peak shortly after initial contact (Greenhalgh et al., 2012; Van den Berghe et al., 2019). The benefit of PTA compared to GRF metrics is that PTA can be easily measured outside of the lab with a wearable accelerometer. Multiple studies link high PTA values to retrospective running injuries (Milner et al., 2006; Pohl et al., 2008; Zifchock et al., 2008). Prospective preliminary data of five runners suggest that runners with a tibial stress fracture tended to have higher PTA values (9.1 g) compared to matched controls (4.7 g; $p = 0.06$) before they sustained an injury (Davis et al., 2004). PTA is often used as a biofeedback variable to decrease impact forces and risk of tibial stress fractures in runners (Clansey et al., 2014; Crowell & Davis, 2011; Crowell et al., 2010) and is even applied in commercially available sensors as an indicator of running injury risk (Runscribe n.d.). Hence, many findings support the idea of using PTA as a surrogate measure for tibial bone forces in running.

Compression forces acting on the tibial bone (F_{tibia}) can be divided into external forces (F_{ext}) caused by the foot contacting the ground and internal forces (F_{int}) caused by the pull of muscles (Romani et al., 2002; Scott & David, 1990). F_{tibia} in the distal tibia can reach values of 10.3 up to 14.3 times BW during running, of which only 18% is caused by F_{ext} (Scott & David, 1990). Most of F_{tibia} is therefore caused by internal forces which reach their maximum compressive action around midstance during running (Burdett, 1982; Glitsch & Baumann, 1997; Matijevich et al., 2019; Sasimontonkul et al., 2007; Scott & David, 1990). Matijevich and colleagues investigated the commonly assumed relationship between GRF metrics (peak vertical GRF around impact and midstance, slope of vertical GRF and GRF impulse) and maximum tibial compression forces ($F_{tibia,max}$) during running (Matijevich et al., 2019). Since GRF does not account for compressive muscle forces, no strong group-level correlation with F_{tibia} was found, although there was high inter-subject variability. Hence, GRF metrics should not be used as indicator of tibial bone forces in running.

Despite the widespread use of PTA as a measure of tibial bone loading and injury risk, PTA (occurring shortly after initial contact) and $F_{tibia,max}$ (occurring around midstance) do not coincide in time. PTA is expected to reflect the contribution of GRF around initial contact to F_{tibia}, however, F_{ext} is only 18% of $F_{tibia,max}$ (Scott & David, 1990). Hence, there is reason to doubt the commonly used PTA as a surrogate for tibial bone loading in running. Therefore, the research question of this study is: How strong is the relationship between PTA and $F_{tibia,max}$ in rearfoot-striking runners during level running at a single speed? It is hypothesised that PTA does not reflect the contribution of F_{int} (i.e., muscle contractions) to $F_{tibia,max}$ and therefore that there are no statistically significant correlations between PTA and $F_{tibia,max}$.

Methods

Participants

Thirteen recreational runners participated in this study. Since internal forces tend to be different for non-rearfoot striking runners, only rearfoot striking runners were included in this study (Almonroeder et al., 2013; Chen et al., 2016; Rooney & Derrick, 2013). Inclusion criteria were: 1) Able to run for 5 min at 14 km/h to prevent possible effects of fatigue; 2) Injury-free for at least 6 months; 3) Self-reported rear-foot strike pattern. One subject was retrospectively excluded from analysis because of a non-rearfoot strike pattern. Data from four females and eight males were included (age: 36.7 ± 12.2 years, height: 178.7 ± 9.6 cm, mass: 74.2 ± 17.7 kg). Subjects ran on average 29.9 ± 19.9 km per week with 15.0 ± 14.9 years of running experience. All participants gave written informed consent before participating in this study. The study protocol was approved by the Ethics Committee Computer and Information Science of the University of Twente (EC-CIS, ref.:RP2021–117).

Measurement systems

Subjects ran on one belt of a dual-belt treadmill with an integrated three-dimensional (3D) force plate (custom Y-mill, Motekforce-Link, Culemborg, The Netherlands). 3D GRFs and ground reaction moments were captured at 2048 Hz. Subjects were equipped with eight IMU sensors (MVN Link, Xsens, Enschede, The Netherlands) capturing at 240 Hz, measuring acceleration (±16 g), angular velocity (±2000 deg/s), and the Earth magnetic field (±1.9 Gauss). Sensors were placed on the sternum and pelvis and bilaterally on the lateral midportion of the thigh, medial surface of the proximal tibia, and on top of the midfoot in the shoes. All sensors had one axis aligned with the longitudinal direction of the associated segment. Sensors were attached to the skin with double-sided tape and covered with stretchable tape (Chadefaux et al., 2019). Subjects wore slightly compressing sleeves to firmly fix the sensors on the tibia to the lower leg.

Measurement protocol

Multiple anthropometric values were measured (body height, hip height, hip width, knee height, ankle height, and shoe length). Subjects wore their own running shoes throughout the experiment. Subjects performed a 5-min warm-up at a self-selected speed on an instrumented treadmill. After the warm-up, an inertial measurement unit (IMU) sensor-to-segment calibration was performed according to the manufacturer's instructions (Xsens Technologies B.V., 2021).

Subjects performed a 90-s running trial at their self-selected step frequency at 12 km/h. Trials started and ended with three jumps on the treadmill to time-synchronise the force plate and IMU data (see section: Temporal synchronisation and spatial alignment) (Day et al., 2021). Since this study was part of a larger experiment, each subject performed a total of nine running trials of 90 s at different speeds (10, 12, and 14 km/h) in random order and with different step frequencies (self-selected and imposed), of which data was not included in further analysis. Subjects had a 3-min break after every trial to minimise possible effects of fatigue.

Data processing

Unless stated otherwise, data were expressed in the global force plate coordinate system ($\Psi^{gl,fp}$) with the X-axis pointing in the running direction, the Y-axis upwards, and the Z-axis to the right. The stance phase of running was defined as the period where the vertical GRF was larger than 20 N (Milner & Paquette, 2015). The stance phase started with initial contact and ended with toe-off. Data were normalised for BW and expressed as a percentage of the stance phase. To exclude the effects of adapting to the treadmill speed, 50 right-leg stance phases between the 40th and 80th second of the running trial were used for analysis. To check if all runners had a rearfoot striking pattern, the mean foot contact angle (i.e., angle between sagittal plane orientation of the foot and the global vertical axis as provided by the IMU-based biomechanical model) at the initial contact was computed for each subject. A mean foot contact angle smaller than 8 degrees (less dorsiflexion results in a smaller angle) was interpreted as a non-rearfoot strike pattern, and these subjects were excluded from further analysis (Altman & Davis, 2012). Data processing and statistics were performed in MATLAB (MathWorks Inc., MA, USA, version 2022a).

IMU data

Sensor orientations were estimated using proprietary filtering based on acceleration, angular velocity, and magnetometer data from the IMUs in the software package Xsens MVN Analyze (version 2020.0.2). Sensor orientations, together with anthropometric measurements, were used to create a scaled biomechanical model of each subject in the same software. Lower body kinematics, 3D coordinates of joint centres, and locations of virtual anatomical landmarks with respect to joint centres were obtained from the scaled biomechanical model (Xsens Technologies B.V., 2021). These IMU-derived data were expressed in either a global IMU-based coordinate system ($\Psi^{gl,imu}$) or a sensor-fixed coordinate system (Ψ^{s}). The forward direction (X-axis) of $\Psi^{gl,imu}$ was determined during the sensor-to-segment calibration and was roughly similar to the running direction in $\Psi^{gl,fp}$.

Force plate data

GRF, ground reaction moments, and centre of pressure (COP) as measured by the force plate (in $\Psi^{gl,fp}$) were low-pass filtered with a third-order recursive Butterworth filter of 15 Hz (Matijevich et al., 2019). Force plate data were then linearly downsampled to 240 Hz to match the sampling frequency of IMU data.

Temporal synchronisation and spatial alignment

A rough estimate of the vertical ground reaction force in running can be made by multiplying vertical pelvis acceleration with BW (Day et al., 2021). Force plate and IMU data can then be time-synchronised by cross-correlating the vertical acceleration of the pelvis segment with the vertical GRF during the first three jumps on the treadmill (Day et al., 2021). Note that BW only functions as a scaling factor and is not necessary for time synchronisation.

To compute F_{tibia}, the sagittal plane ankle moment (M_{ankle}) and the GRF moment arm with respect to the ankle joint centre was required (see section: Tibial compression force). To compute the GRF moment arm, IMU-derived data (expressed in $\Psi^{gl,imu}$) needed to be

transformed to $\Psi^{gl,fp}$. First, the orientation of $\Psi^{gl,imu}$ was rotated to match the orientation of $\Psi^{gl,fp}$ using the running direction (positive X-axis). The IMU-based biomechanical model cannot distinguish between stationary (i.e., on a treadmill) and overground running, which resulted in a displacement of the pelvis segment in $\Psi^{gl,imu}$ of about 250 m during each trial, predominantly in the X-axis. A least-squares line was fitted through the forward and sideward pelvis displacement in $\Psi^{gl,imu}$ and the angle between these lines was used to rotate all IMU-derived data from $\Psi^{gl,imu}$ to $\Psi^{gl,fp}$.

The origin of $\Psi^{gl,imu}$ was then translated to match $\Psi^{gl,fp}$ during each step to be able to estimate the GRF moment arm and compute M_{ankle}. Since F_{tibia} is computed with a 2D model, only spatial alignment of data in the forward direction (X-axis) was required. The COP trajectory was provided by the force plate in $\Psi^{gl,fp}$. In rearfoot striking runners on a treadmill, the forward trajectory of COP (COP_x) over the surface of the foot was expected to be similar. Therefore, it was assumed that the percentage of the stance phase at which COP_x crossed the fifth metatarsal marker ($MT5_x$) would be similar between strides and subjects. The IMU-based scaled biomechanical model provided virtual marker locations of the heel and MT5 with respect to the ankle joint center. These virtual marker locations were modeled based on the foot length of participants. The mean percentage of the stance phase at which COP_x crossed $MT5_x$ in rearfoot runners was then used to spatially align $\Psi^{gl,imu}$ with $\Psi^{gl,fp}$ in the X-direction during each stride, see Figure 1. A published dataset of six rearfoot striking runners running at eight different speeds was used to test this method and to obtain the mean percentage of the stance phase at which COP_x crossed

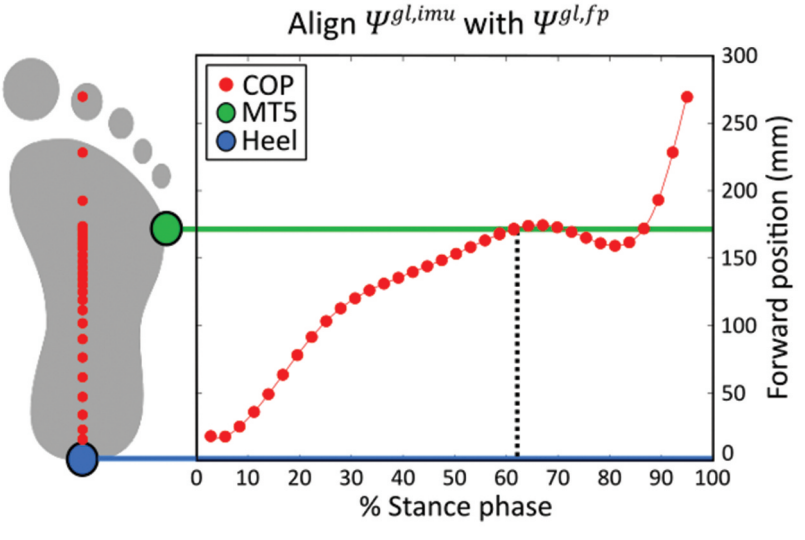

Figure 1. Visualization of spatial alignment method for $\Psi^{gl,imu}$ and $\Psi^{gl,fp}$ for a representative subject. The mean percentage of the stance phase at which the center of pressure (COP) crosses the fifth metatarsal marker (*MT5*) in the forward direction (X-axis) is used to align $\Psi^{gl,imu}$ and $\Psi^{gl,fp}$. COP and *MT5* positions with respect to the heel marker are shown. COP data was downsampled for visualization purposes and only the forward position of COP is aligned and shown. This figure was inspired by Figure 1 of (Fuchioka et al., 2015).

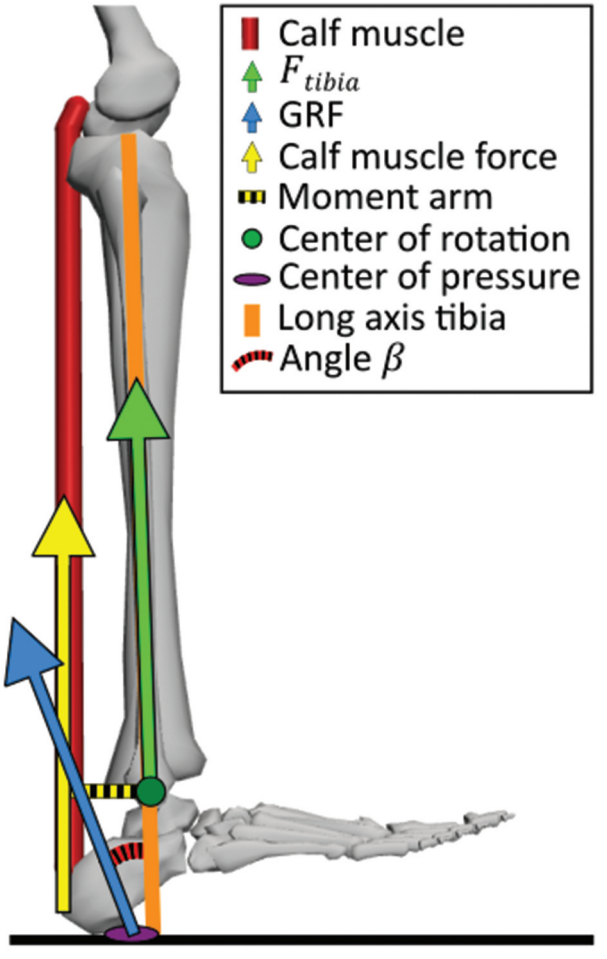

Figure 2. Visualization of the 2D lower leg model to estimate tibial compression forces. Calf muscle = combination of the soleus, gastrocnemius medialis and lateralis muscles; r_{at}= Achilles tendon moment arm relative to the ankle joint center; GRF = ground reaction force; Center of rotation = center of rotation of the ankle joint; Angle β = Angle between long axis of tibia and ground reaction force vector in the sagittal plane.

$MT5_x$ [32]. This mean percentage at which COP_x crossed $MT5_x$ was then applied to all steps from all subjects from the online dataset. The error of this alignment method was quantified by computing the absolute distance between $MT5_x$ and COP_x at the group-mean percentage of the stance phase were $MT5_x$ crossed COP_x. A full description of the analyses of the online dataset can be found in the Appendix.

Tibial compression force (F_{tibia})

F_{tibia} was defined as the axial compression force on the distal end of the tibia and is equal to the ankle compression force (Matijevich et al., 2019, 2020; Sasimontonkul et al., 2007; Scott & David, 1990), see Figure 2. F_{tibia} is computed according to a 2D (sagittal plane) lower limb model which sums the ankle joint reaction force caused by GRF (F_{ext}) and an

estimate of compression forces on the tibia exerted by the soleus, gastrocnemius medialis, and lateralis plantar flexor muscles (F_{int}) while ignoring contributions of other muscles (Scott & David, 1990).

$$F_{tibia}(t) = F_{ext}(t) + F_{int}(t) \tag{1}$$

The mass and inertia of the foot were assumed to be negligible (Matijevich et al., 2019, 2020; Scott & David, 1990). F_{ext} was therefore set equal to GRF in the axial direction of the tibia, but GRF was low-pass filtered with a 45 Hz ($\overrightarrow{GRF}^{*}$) instead of a 15 Hz cut-off frequency to allow representation of the heel impact in F_{ext} (Matijevich et al., 2019; Scott & David, 1990):

$$F_{ext}(t) = \left|\overrightarrow{GRF}^{*}(t)\right| * \cos\beta(t) \tag{2}$$

where β represents the angle between $\overrightarrow{GRF}^{*}$ and the orientation of the tibial segment (obtained from IMU-based biomechanical model) in the sagittal plane. F_{int} is computed as M_{ankle} divided by the Achilles tendon moment arm relative to the ankle joint centre (r_{at}), which was assumed to be constant and 0.05 m (Farris & Sawicki, 2012; Honert & Zelik, 2016; Matijevich et al., 2019, 2020):

$$F_{int}(t) = \frac{M_{ankle}}{r_{at}} = \frac{COP_{x,ankle} * GRF_z(t)}{0.05} \tag{3}$$

where $COP_{x,ankle}$ represent the forward COP position with respect to the ankle joint centre obtained from the scaled biomechanical model and is an estimate of the GRF moment arm relative to the ankle joint centre. M_{ankle} was estimated by multiplying $COP_{x,ankle}$ with the vertical GRF (GRF_z). This computation of M_{ankle} assumes that solely the plantar flexors contribute to F_{int} during the stance phase and that there is no co-contraction between plantar and dorsi flexors during the stance phase (Matijevich et al., 2019, 2020; Scott & David, 1990).

Peak tibial acceleration

The acceleration of the tibial sensor, including gravity ($\vec{a}_{tibia}$) expressed in Ψ^{s}, was filtered with a fourth-order Butterworth recursive lowpass filter of 60 Hz to minimise noise (Sheerin et al., 2019). PTA was defined as the peak acceleration in the axial direction of the tibial sensor in the local tibial sensor coordinate system, similar to (Clansey et al., 2014; Lucas-Cuevas et al., 2015; Reenalda et al., 2019).

Statistical analysis

To test if PTA correlates with $F_{tibia,max}$ in running on level ground at a single speed, Pearson's correlation coefficients (r) were computed for each participant independently, after which the group mean correlation was computed. Correlation coefficients were based on 50 right leg PTA and $F_{tibia,max}$ values for each subject. Correlations were interpreted as very strong $r = \pm(0.90, 1.00)$, strong for $r = \pm(0.70, 0.89)$, moderate for $r = \pm(0.40, 0.69)$,

weak for $r = \pm(0.20, 0.39)$ and very weak for $r = \pm(0.00, 0.19)$ (Evans, 1996). The level of statistical significance was set to an alpha of 0.05. The influence of an offset in aligning $\Psi^{gl,imu}$ with $\Psi^{gl,fp}$ on the conclusion of this study was assessed by introducing an additional error of 10, 20, and 30 mm to the alignment of $\Psi^{gl,imu}$ and $\Psi^{gl,fp}$ and recomputing the correlation between PTA and $F_{tibia,max}$ with these offsets.

Results

$F_{tibia,max}$ was estimated to be, on average 7.6 ± 0.6 BW with a range of 6.5 to 8.7 BW, see Table 1 and Figure 3. The within-subject range of $F_{tibia,max}$ was on average 1.6 BW. Mean PTA was 7.8 ± 1.6 g and ranged from 4.9 up to 10.1 g. The within-subject range of PTA was on average 3.3 g. On a group level, PTA and $F_{tibia,max}$ showed a very weak correlation coefficient of 0.04 ± 0.14 with a range of −0.15 up to 0.28 (very weak to weak). No significant correlations between PTA and $F_{tibia,max}$ were found for any of the runners, see Figure 4.

To validate the method to spatially align $\Psi^{gl,imu}$ with $\Psi^{gl,fp}$ during each step, to be able to compute the GRF moment arm, an online dataset was used (Matijevich et al., 2019). On average, COP crossed the MT5 marker in the forward direction at 62 ± 12% of the gait cycle with a range of 47% to 85%, see Table 2. Within-subject variability was small, while between-subject variability was larger. The mean absolute error introduced by this alignment method was 12 ± 15 mm with a range of 4–28 mm.

The effect of a possible error in tibial force estimates caused by the alignment method of $\Psi^{gl,imu}$ with $\Psi^{gl,fp}$on the conclusion of this study was investigated by applying an additional alignment offset in the forward direction impacting the GRF moment arm estimate, see Table 3. An additional alignment offset influenced the estimation of F_{int} and $F_{tibia,max}$, however the correlation between $F_{tibia,max}$ and PTA remained very weak for all imposed offsets.

Table 1. Mean maximum values. Range refers to the minimum and maximum average subject values (coloured dots in Figure 4). GRF_{max} = Maximum vertical ground reaction force; $M_{ankle,max}$ = Maximum ankle moment; $F_{ext,max}$ = Maximum external force; $F_{int,max}$ = Maximum internal force; $F_{tibia,max}$ = Maximum tibial force; PTA = Peak tibial acceleration; r = correlation coefficient; BW = body weight; g = gravitational acceleration; SD = standard deviation.

	Mean ± SD	Range
GRF_{max} (BW)	2.4 ± 0.2	2.1–2.7
$M_{ankle,max}(\frac{Nm}{kg})$	0.3 ± 0.0	0.2–0.3
$F_{ext,max}$ (BW)	2.4 ± 0.2	2.1–2.8
$F_{int,max}$ (BW)	5.3 ± 0.6	4.5–6.2
$F_{tibia,max}$ (BW)	7.6 ± 0.6	6.5–8.7
PTA (g)	7.8 ± 1.6	4.9–10.1
Correlation PTA - F_{tibia} (r)	0.04 ± 0.14	-0.15–+0.28

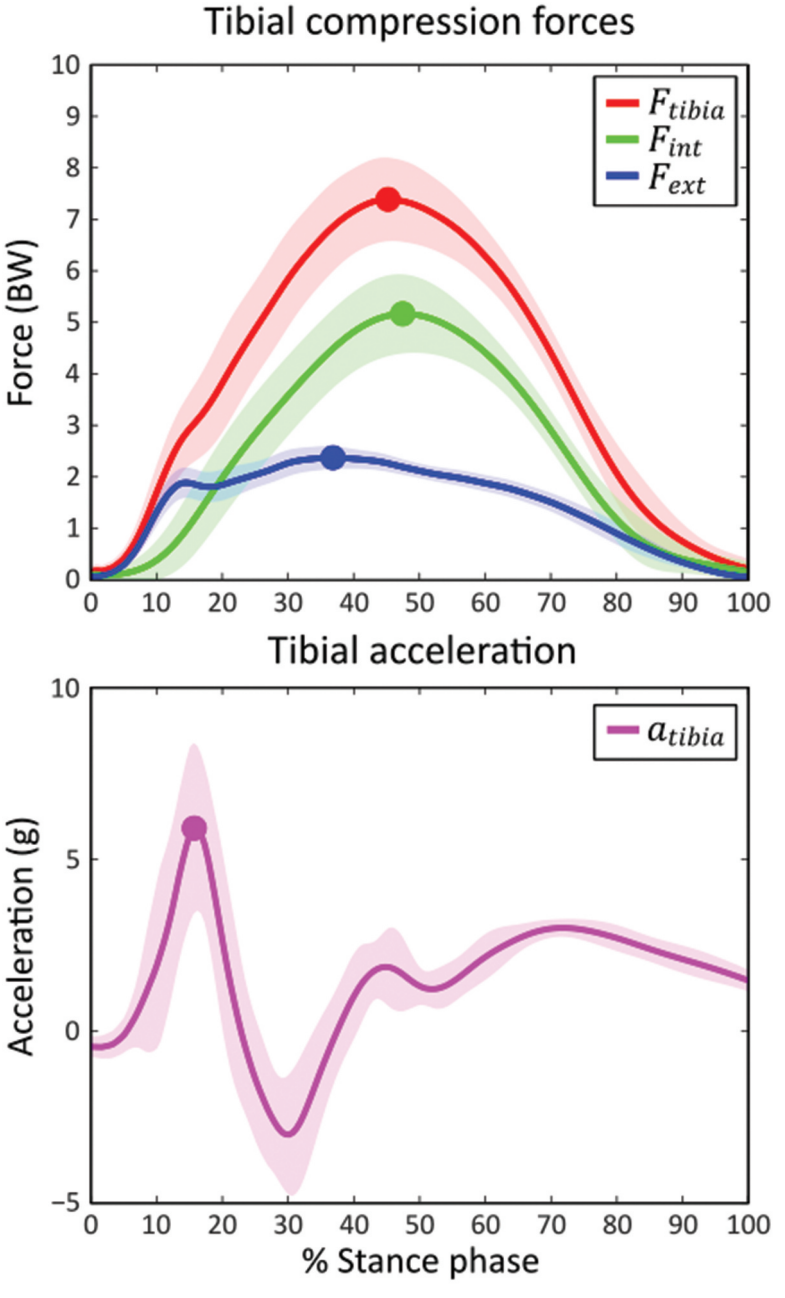

Figure 3. Group average estimated tibial forces (top figure) and axial tibial acceleration (bottom figure) as a percentage of the stance phase. Dots represent maximum values for estimated tibial forces and tibial acceleration during the stance phase. Shaded areas represent the standard deviation around the group mean. F_{tibia} = tibial compression force; F_{int} = Internal component of tibial compression force (i.e., caused by muscle contractions); F_{ext} = external component of tibial compression force (i.e., caused by ground reaction force); a_{tibia} = tibial acceleration in the axial direction of the tibial sensor; BW = body weight; g = gravitational acceleration.

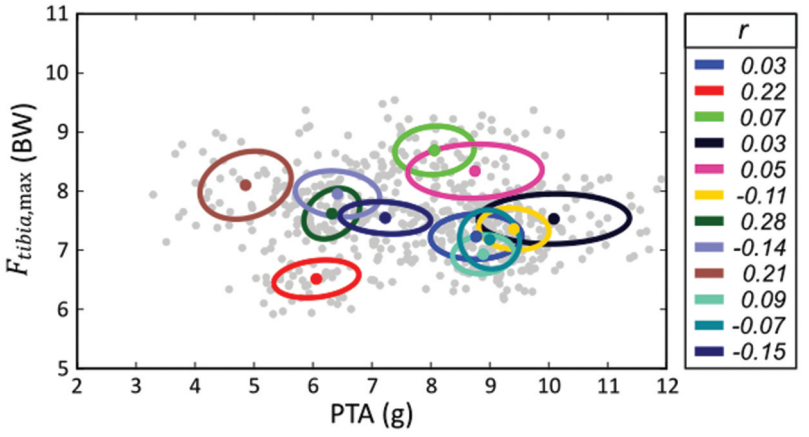

Figure 4. Scatterplot of PTA and estimated $F_{tibia,max}$ values for all 50 strides of all subjects (light grey dots). Coloured dots represent the mean PTA and $F_{tibia,max}$ for each subject. Coloured ellipses represent the standard deviation ellipse for all individual runners. The legend shows the correlation coefficients (r) between PTA and $F_{tibia,max}$.

Table 2. Results from validating the spatial alignment method on an online dataset. The second column shows the percentage of the stance phase at which the centre of pressure in the forward direction (COP_x) crossed the marker of the fifth metatarsal ($MT5_x$). The third column shows the absolute mean error in spatial alignment introduced by assuming that COP_x always crossed $MT5_x$ at 62% of the stance phase.

Subject	*COP* crossing *MT5* (% stance phase)	Absolute mean error (mm)
1	47 ± 2	28 ± 3
2	59 ± 3	4 ± 3
4	85 ± 10	16 ± 3
5	56 ± 4	9 ± 5
6	68 ± 3	5 ± 2
7	68 ± 6	14 ± 9
10	56 ± 2	8 ± 3
Group mean	62 ± 12	12 ± 15

Table 3. Influence of additional alignment offset between $\psi^{gl,imu}$ and $\psi^{gl,fp}$ on the estimated tibial forces and the correlation between PTA and $F_{tibia,max}$. Columns represent the introduced translation error in the forward direction of $\psi^{gl,imu}$ with respect to $\psi^{gl,fp}$ for each step.

	−30 mm	−20 mm	−10 mm	0 mm	+10 mm	+20 mm	+30 mm
$F_{ext,max}$ (BW)	2.4 ± 0.2	2.4 ± 0.2	2.4 ± 0.2	2.4 ± 0.2	2.4 ± 0.2	2.4 ± 0.2	2.4 ± 0.2
$F_{int,max}$ (BW)	4.0 ± 0.5	4.4 ± 0.5	4.9 ± 0.6	5.3 ± 0.6	5.8 ± 0.6	6.3 ± 0.6	6.8 ± 0.6
$F_{tibia,max}$ (BW)	6.2 ± 0.6	6.6 ± 0.6	7.1 ± 0.6	7.6 ± 0.6	8.1 ± 0.6	8.5 ± 0.6	9.0 ± 0.7
Correlation PTA -$F_{tibia,max}$ (r)	0.04 ± 0.14	0.04 ± 0.14	0.04 ± 0.14	0.04 ± 0.14	0.04 ± 0.15	0.04 ± 0.15	0.05 ± 0.15

Discussion and implications

This research aimed to investigate the strength of the relationship between PTA, a commonly used measure for tibial bone loading, and estimated $F_{tibia,max}$ during treadmill running. This study showed a very weak correlation ($r = 0.04 \pm 0.14$) between PTA and $F_{tibia,max}$ in rearfoot striking runners on a treadmill at a single running speed. The hypothesis that there would be no statistically significant correlations between PTA and $F_{tibia,max}$ was accepted. On a group level, the very weak correlation between PTA and $F_{tibia,max}$ cannot be considered relevant for estimating tibial bone loading based on PTA. The weak correlations between PTA and $F_{tibia,max}$ are expected to be caused by the inability of PTA to reflect internal compressive forces from muscle contractions and the mis-timing between PTA (shortly after initial contact) and $F_{tibia,max}$ (around mid-stance). The use of PTA as a surrogate measure for $F_{tibia,max}$ during treadmill running is therefore not supported by the findings of this study.

PTA and GRF reflect the effect of external forces on the body during running. GRF represents the effect of external forces during the complete stance phase, while PTA mostly reflects the impact peak that travels up the leg caused by the foot hitting the ground at the start of the stance phase. The contribution of F_{ext} to $F_{tibia,max}$ is only about 18–30%, while the remainder is caused by F_{int} (Scott & David, 1990). PTA, GRF loading rate, and GRF impact peak are often used as surrogate measures for each other and for tibial bone loading (Bigelow et al., 2013; Chadefaux et al., 2019; García-Pérez et al., 2014; Lafortune et al., 1996; Lucas-Cuevas et al., 2015; Milner et al., 2006; Mizrahi et al., 2000; Zadpoor & Nikooyan, 2011). Previously, Matijevich et al. (Matijevich et al., 2019) showed that the slope of the vertical GRF and impact peak did not strongly correlate with F_{tibia}. Hence, the contribution of the high impact peak shortly after initial contact towards tibial stress fracture injury risk has been challenged before (Hamill et al., 2018; Loundagin et al., 2018) but not in relation to PTA assessed using an IMU on the tibia, although this relation has been often assumed (Bigelow et al., 2013; Chadefaux et al., 2019; García-Pérez et al., 2014; Lafortune et al., 1996; Lucas-Cuevas et al., 2015; Milner et al., 2006; Mizrahi et al., 2000; Zadpoor & Nikooyan, 2011). No strong correlations between the slope of the vertical GRF, GRF impact peak, PTA, and tibial bone loading have been found in this study or in other literature (Matijevich et al., 2019; Van den Berghe et al., 2019), indicating that these metrics should not be used as surrogate measures for each other.

A group mean value for PTA of 7.8 ± 1.6 g was found, which is well within the expected range when running at 12 km/h (Milner et al., 2020; Sheerin et al., 2019; Van den Berghe et al., 2019). $F_{tibia,max}$ in this study was estimated to be 7.6 ± 0.6 BW on average, which is similar to studies in which subjects ran at a similar speed (Matijevich et al., 2020) and falls between values reported for lower (Chen et al., 2016) and higher speeds (Burdett, 1982; Sasimontonkul et al., 2007; Scott & David, 1990). $F_{tibia,max}$ increases with running speed (Edwards et al., 2010). Values for $F_{int,max}$, also called plantar flexor forces or Achilles tendon forces, reported in the literature were similar to our findings, respectively, 5.7 ± 1.5 versus 5.3 ± 0.6 BW (Kernozek et al., 2017). Comparable values for F_{int} of 5.1 ± 0.9 BW (Sinclair, 2014) when running at 14.4 km/h and 6.1 ± 0.6 (Almonroeder et al., 2013) when running at 13 km/h were found in the literature. In vivo values for $F_{int,max}$ of 3750 N at 14 km/h were found with a buckle transducer (Komi, 1990). These findings are only slightly lower than what we found (3914 ± 1094 N). Values for $F_{ext,max}$ from our study (2.4 ± 0.2 BW) were

higher than found in the literature (1.6–2.0 BW) (Sasimontonkul et al., 2007; Scott & David, 1990) at similar speeds. Overall, PTA and estimated tibial force values of this study are in line with the literature.

A simple 2D lower leg model was used to estimate F_{tibia} of the distal third of the tibial bone (Scott & David, 1990). This model assumes that only the gastrocnemius medialis, lateralis, and soleus contribute to F_{int}, that there is no co-activation of dorsiflexor muscles or other plantarflexor muscles, no influence of biarticular muscles and neglects the mass and inertia of the foot. These assumptions likely result in an underestimation of true F_{int} at similar speeds due to co-activation of dorsiflexor muscles and contribution of smaller plantarflexor muscles. F_{ext} is likely overestimated in the simple 2D lower leg model since the mass and inertia of the foot dampens GRF while the model assumes that the full GRF acts on the ankle joint. Multiple studies used more elaborate models to estimate F_{tibia} that included dorsiflexor muscles and smaller plantarflexor muscles (Burdett, 1982; Kernozek et al., 2017; Sasimontonkul et al., 2007). They found that during 20–90% of the stance phase, mostly the gastrocnemius medialis, lateralis, and soleus were active with only little contributions (max 0.3 BW per muscle) from other plantar or dorsiflexor muscles (Sasimontonkul et al., 2007). When co-activation occurred, this was mostly during the start and end of the stance phase while $F_{tibia,max}$ occurs around midstance. The simple 2D lower leg model has been shown to provide $F_{int,max}$ in running that were similar to an extensive musculoskeletal model using 300 muscles with static optimisation, respectively, 5.7 ± 0.6 and 5.5 ± 1.4 BW (Kernozek et al., 2017). A 2D versus a 3D lower leg model to compute $F_{tibia,max}$ and $F_{int,max}$ provided similar results for both models (Burdett, 1982). Hence, using a simple or more elaborate model of the lower leg to estimate F_{tibia} is not expected to influence the conclusion of this study.

A new method was developed, validated, and applied to spatially align force plate and IMU data in the forward direction to be able to estimate the GRF moment arm relative to the ankle joint centre. Validation was performed on an online dataset and showed an absolute misalignment error of 12 ± 15 mm in the forward direction (Matijevich et al., 2019). To ascertain that an error of this magnitude would not affect the conclusion of this study, an additional offset between $\Psi^{gl,imu}$ and $\Psi^{gl,fp}$ was added (i.e., affecting the GRF moment arm relative to the ankle joint centre and thus M_{ankle}, F_{int} and F_{tibia}) and the correlation between PTA and $F_{tibia,max}$ was computed. This analysis showed that despite some uncertainty regarding the exact alignment of $\Psi^{gl,imu}$ and $\Psi^{gl,fp}$, all alignment offsets (of up to 30 mm) resulted in a very weak correlation ($r = 0.04$–0.05) and did not influence the conclusion of this study.

This study focused on the relationship between tibial compression forces and one-dimensional axial tibial sensor acceleration. Besides compression forces, bending and shear forces on the tibia might play a role in the development of stress fractures (Burdett, 1982; Glitsch & Baumann, 1997; Sasimontonkul et al., 2007; Scott & David, 1990). However, there is no reason to expect that PTA, measured in the axial direction of the tibial bone, would correlate better with bending or shear forces than with axial compression forces. Additionally, these bending and shear forces are of a smaller magnitude (max 1.2 BW) and work in different directions than maximum axial compression forces (Sasimontonkul et al., 2007). The axial compared to the resultant tibial acceleration was investigated in this study due to its demonstrated relationship with injuries (Sheerin et al., 2019) and possibly a stronger correlation with tibial compression forces.

The difference between axial and resultant PTA is caused by acceleration components in the forward and sideward directions, while these are not expected to contribute to axial compression forces. Hence, the correlation between the resultant PTA and $F_{tibia,max}$ is expected to be lower than between the axial PTA and $F_{tibia,max}$.

The results of this study are based on a relatively small sample of 12 subjects. None of the runners showed a significant correlation between PTA and $F_{tibia,max}$. Increasing the sample size of this study would likely not affect the conclusion that there is no clinically relevant correlation between PTA and $F_{tibia,max}$ on a group level.

Measurements were performed on an indoor instrumented treadmill. However, the effect of running surface on PTA is unclear (Fu et al., 2015; García-Pérez et al., 2014; Milner et al., 2020; Montgomery et al., 2016). In-vivo axial tibial compression strains were lower (Milgrom et al., 2003) while modelled F_{int} were higher in treadmill versus overground running (Willy et al., 2016). Without further understanding of the effect of running surface on PTA and tibial forces, the results of this study cannot be generalised to overground running without additional validation.

This study showed that there is only a very weak and non-significant correlation between PTA and $F_{tibia,max}$ during treadmill running in rearfoot-striking runners, which cannot be considered relevant for estimating tibial bone loading based on PTA. Hence, PTA as an indicator for $F_{tibia,max}$ and tibial stress fractures, as often used in the literature and commercial products, is not supported by scientific data. PTA might be an indicator of other running-related injuries, although the relation between PTA and tibial stress fracture risk is most referred to in the literature (Clansey et al., 2014; Crowell & Davis, 2011; Milner et al., 2006). Future research should focus on a surrogate measure for tibial bone loading, which includes the contribution of F_{int}. The plantar flexor muscles are the largest contributors to F_{tibia} (Kernozek et al., 2017) and the magnitude of ankle power generation is directly related to running speed (Novacheck, 1998). Therefore, 3D acceleration of the pelvis (i.e., close to the centre of mass) might reflect plantar flexor forces during running, and thus the contribution of F_{int} to F_{tibia}.

Conclusion

A very weak but non-significant correlation between PTA and $F_{tibia,max}$ in treadmill running at a single speed on level ground was found for rearfoot-striking runners. Compression forces on the tibia are composed of both F_{int} (i.e., muscle contractions) and F_{ext} (i.e., GRF). PTA is unable to reflect the contribution of muscle contractions to F_{tibia}. Hence, the assumed link between PTA and tibial bone loading ($F_{tibia,max}$), and between PTA and the risk of tibial stress fractures during treadmill running is not supported by the results of this study. Further research should focus on validating these findings in overground running and the development of a surrogate measure for F_{tibia} which reflects both F_{int} and F_{ext}.

Acknowledgment

The authors would like to thank Bouke Scheltinga and Hazal Usta for their assistance during the data collection process. Furthermore, the authors would like to thank all participants for their willingness and enthusiasm to participate in this study.

Disclosure statement

No potential conflict of interest was reported by the author(s).

Funding

This work was supported by EFRO OP Oost under [Grant 0784].

References

Almonroeder, T., Willson, J. D., & Kernozek, T. W. (2013). The effect of foot strike pattern on achilles tendon load during running. *Annals of Biomedical Engineering*, *41*(8), 1758–1766. https://doi.org/10.1007/s10439-013-0819-1

Altman, A. R., & Davis, I. S. (2012). A kinematic method for footstrike pattern detection in barefoot and shod runners. *Gait & Posture*, *35*(2), 298–300. https://doi.org/10.1016/j.gaitpost.2011.09.104

Bigelow, E. M. R., Elvin, N. G., Elvin, A. A., & Arnoczky, S. P. (2013). Peak impact accelerations during track and treadmill running. *Journal of Applied Biomechanics*, *29*(5), 639–644. https://doi.org/10.1123/jab.29.5.639

Burdett, R. G. (1982). Forces predicted at the ankle during running. *Medicine & Science in Sports & Exercise*, *14*(4), 308–316. https://doi.org/10.1249/00005768-198204000-00010

Chadefaux, D., Gueguen, N., Thouze, A., & Rao, G. (2019). 3D propagation of the shock-induced vibrations through the whole lower-limb during running. *Journal of Biomechanics*, *96*, 109343. https://doi.org/10.1016/j.jbiomech.2019.109343

Chen, T. L., An, W. W., Chan, Z. Y. S., Au, I. P. H., Zhang, Z. H., & Cheung, R. T. H. (2016). Immediate effects of modified landing pattern on a probabilistic tibial stress fracture model in runners. *Clinical Biomechanics*, *33*, 49–54. https://doi.org/10.1016/j.clinbiomech.2016.02.013

Clansey, A. C., Hanlon, M., Wallace, E. S., Nevill, A., & Lake, M. J. (2014). Influence of tibial shock feedback training on impact loading and running economy. *Medicine & Science in Sports & Exercise*, *46*(5), 973–981. https://doi.org/10.1249/MSS.0000000000000182

Crowell, H. P., & Davis, I. S. (2011). Gait retraining to reduce lower extremity loading in runners. *Clinical Biomechanics*, *26*(1), 78–83. https://doi.org/10.1016/j.clinbiomech.2010.09.003

Crowell, H. P., Milnert, C. E., Hamill, J., & Davis, I. S. (2010). Reducing impact loading during running with the use of real-time visual feedback. *Journal of Orthopaedic & Sports Physical Therapy*, *40*(4), 206–213. https://doi.org/10.2519/jospt.2010.3166

Davis, I., Milner, C. E., & Hamill, J. (2004). Does increased loading during running lead to tibial stress fractures? A prospective study. *Medicine & Science in Sports & Exercise*, *36*(Supplement), S58. https://doi.org/10.1249/00005768-200405001-00271

Day, E. M., Alcantara, R. S., McGeehan, M. A., Grabowski, A. M., & Hahn, M. E. (2021). Low-pass filter cutoff frequency affects sacral-mounted inertial measurement unit estimations of peak vertical ground reaction force and contact time during treadmill running. *Journal of Biomechanics*, *119*, 110323. https://doi.org/10.1016/j.jbiomech.2021.110323

Edwards, W. B. (2018). Modeling overuse injuries in sport as a mechanical fatigue phenomenon. *Exercise and Sport Sciences Reviews*, *46*(4), 224–231. https://doi.org/10.1249/JES.0000000000000163

Edwards, W., Taylor, D., Rudolphi, T. J., Gillette, J. C., & Derrick, T. R. (2010). Effects of running speed on a probabilistic stress fracture model. *Clinical Biomechanics*, *25*(4), 372–377. https://doi.org/10.1016/j.clinbiomech.2010.01.001

Evans, J. D. (1996). *Straightforward statistics for the behavioral sciences*. Thomson Brooks/Cole Publishing Co.

Farris, D. J., & Sawicki, G. S. (2012). Human medial gastrocnemius force-velocity behavior shifts with locomotion speed and gait. *Proceedings of the National Academy of Sciences of the United States of America*, *109*(3), 977–982. https://doi.org/10.1073/pnas.1107972109

Fuchioka, S., Iwata, A., Higuchi, Y., Miyake, M., Kanda, S., & Nishiyama, T. (2015). The forward velocity of the center of pressure in the midfoot is a major predictor of gait speed in older adults. *International Journal of Gerontology*, *9*(2), 119–122. https://doi.org/10.1016/j.ijge.2015.05.010

Fu, W., Fang, Y., Liu, D. M. S., Wang, L., Ren, S., & Liu, Y. (2015). Surface effects on in-shoe plantar pressure and tibial impact during running. *Journal of Sport and Health Science*, *4*(4), 384–390. https://doi.org/10.1016/j.jshs.2015.09.001

García-Pérez, J. A., Pérez-Soriano, P., Llana Belloch, S., Lucas-Cuevas, Á. G., & Sánchez-Zuriaga, D. (2014). Effects of treadmill running and fatigue on impact acceleration in distance running. *Sports Biomechanics*, *13*(3), 259–266. https://doi.org/10.1080/14763141.2014.909527

Glitsch, U., & Baumann, W. (1997). The three-dimensional determination of internal loads in the lower extremity. *Journal of Biomechanics*, *30*(11–12), 1123–1131. https://doi.org/10.1016/S0021-9290(97)00089-4

Greenhalgh, A., Sinclair, J., Protheroe, L., & Chockalingam, N. (2012). Predicting impact shock magnitude: Which ground reaction force variable should we use? *ISSN International Journal of Sports Science and Engineering*, *6*(4), 1750–9823.

Hamill, J., Boyer, K. A., & Weir, G. (2018). A paradigm shift is necessary to relate running injury risk and footwear design – comment on Nigg et al. *Current Issues in Sport Science*, *3*, 1–3. https://doi.org/10.15203/ciss_2018.104

Harrast, M. A., & Colonno, D. (2010). Stress fractures in runners. *Clinics in Sports Medicine*, *29*(3), 399–416. https://doi.org/10.1016/j.csm.2010.03.001

Honert, E. C., & Zelik, K. E. (2016). Inferring muscle-tendon unit power from ankle joint power during the push-off phase of human walking: Insights from a multiarticular EMG-driven model. *Plos One*, *11*(10), 1–16. https://doi.org/10.1371/journal.pone.0163169

James, S., Bates, B., & Osternig, L. (1978). Injuries to runners. *American Journal of Sports Medicine*, *6*(2), 40–50. https://doi.org/10.1177/036354657800600202

Kernozek, T., Gheidi, N., & Ragan, R. (2017). Comparison of estimates of Achilles tendon loading from inverse dynamics and inverse dynamics-based static optimisation during running. *Journal of Sports Sciences*, *35*(21), 2073–2079. https://doi.org/10.1080/02640414.2016.1255769

Komi, P. V. (1990). Relevance of in vivo force measurements to human biomechanics. *Journal of Biomechanics*, *23*(SUPPL. 1), 23–34. https://doi.org/10.1016/0021-9290(90)90038-5

Lafortune, M. A., Lake, M. J., & Hennig, E. M. (1996). Differential shock transmission response of the human body to impact severity and lower limb posture. *Journal of Biomechanics*, *29*(12), 1531–1537. https://doi.org/10.1016/S0021-9290(96)80004-2

Lanyon, L. E., Hampson, W. G. J., Goodship, A. E., & Shah, J. S. (1975). Bone deformation recorded in vivo from strain gauges attached to the human tibial shaft. *Acta Orthopaedica*, *46*(2), 256–268. https://doi.org/10.3109/17453677508989216

Loundagin, L. L., Schmidt, T. A., & Brent Edwards, W. (2018). Mechanical fatigue of bovine cortical bone using ground reaction force waveforms in running. *Journal of Biomechanical Engineering*, *140*(3), 1–5. https://doi.org/10.1115/1.4038288

Lucas-Cuevas, A. G., Priego-Quesada, J. I., Aparicio, I., Giménez, J. V., Llana-Belloch, S., & Pérez-Soriano, P. (2015). Effect of 3 weeks use of compression garments on stride and impact shock during a fatiguing run. *International Journal of Sports Medicine*, *36*(10), 826–831. https://doi.org/10.1055/s-0035-1548813

Matijevich, E. S., Branscombe, L. M., Scott, L. R., & Zelik, K. E. (2019). Ground reaction force metrics are not strongly correlated with tibial bone load when running across speeds and slopes: Implications for science, sport and wearable tech. *Plos One*, *14*(1), 1–19. https://doi.org/10.1371/journal.pone.0210000

Matijevich, E. S., Scott, L. R., Volgyesi, P., Derry, K. H., & Zelik, K. E. (2020). Combining wearable sensor signals, machine learning and biomechanics to estimate tibial bone force and damage during running. *Human Movement Science*, *74*(December 2019), 102690. https://doi.org/10.1016/j.humov.2020.102690

McBryde, A. M. (1985). Stress fractures in runners. *American Journal of Sports Medicine*, *4*(4), 737–752. https://doi.org/10.1016/S0278-5919(20)31190-X

Milgrom, C., Finestone, A., Levi, Y., Simkin, A., Ekenman, I., Mendelson, S., Millgram, M., Nyska, M., Benjuya, N., & Burr, D. (2000). Do high impact exercises produce higher tibial strains than running? *British Journal of Sports Medicine*, *34*(3), 195–199. https://doi.org/10.1136/bjsm.34.3.195

Milgrom, C., Finestone, A., Segev, S., Olin, C., Arndt, T., & Ekenman, I. (2003). Are overground or treadmill runners more likely to sustain tibial stress fracture? *British Journal of Sports Medicine*, *37*(2), 160–163. https://doi.org/10.1136/bjsm.37.2.160

Milner, C. E., Ferber, R., Pollard, C. D., Hamill, J., & Davis, I. S. (2006). Biomechanical factors associated with tibial stress fracture in female runners. *Medicine & Science in Sports & Exercise*, *38*(2), 323–328. https://doi.org/10.1249/01.mss.0000183477.75808.92

Milner, C. E., Hawkins, J. L., & Aubol, K. G. (2020). Tibial acceleration during running is higher in field testing than indoor testing. *Medicine and Science in Sports and Exercise*, *52*(6), 1361–1366. https://doi.org/10.1249/MSS.0000000000002261

Milner, C. E., & Paquette, M. R. (2015). A kinematic method to detect foot contact during running for all foot strike patterns. *Journal of Biomechanics*, *48*(12), 3502–3505. https://doi.org/10.1016/j.jbiomech.2015.07.036

Mizrahi, J., Verbitsky, O., & Isakov, E. (2000). Fatigue-related loading imbalance on the shank in running: A possible factor in stress fractures. *Annals of Biomedical Engineering*, *28*(4), 463–469. https://doi.org/10.1114/1.284

Montgomery, G., Abt, G., Dobson, C., Smith, T., & Ditroilo, M. (2016). Tibial impacts and muscle activation during walking, jogging and running when performed overground, and on motorised and non-motorised treadmills. *Gait & Posture*, *49*, 120–126. https://doi.org/10.1016/j.gaitpost.2016.06.037

Novacheck, T. F. (1998). The biomechanics of running. *Gait & Posture*, *7*(1), 77–95. https://doi.org/10.1016/S0966-6362(97)00038-6

Pohl, M. B., Mullineaux, D. R., Milner, C. E., Hamill, J., & Davis, I. S. (2008). Biomechanical predictors of retrospective tibial stress fractures in runners. *Journal of Biomechanics*, *41*(6), 1160–1165. https://doi.org/10.1016/j.jbiomech.2008.02.001

Reenalda, J., Maartens, E., Buurke, J. H., & Gruber, A. H. (2019). Kinematics and shock attenuation during a prolonged run on the athletic track as measured with inertial magnetic measurement units. *Gait & Posture*, *68*(January 2018), 155–160. https://doi.org/10.1016/j.gaitpost.2018.11.020

Romani, W. A., Gieck, J. H., Perrin, D. H., Saliba, E. N., & Kahler, D. M. (2002). Mechanisms and management of stress fractures in physically active persons. *Journal of Athletic Training*, *37*(3), 306–314.

Rooney, B. D., & Derrick, T. R. (2013). Joint contact loading in forefoot and rearfoot strike patterns during running. *Journal of Biomechanics*, *46*(13), 2201–2206. https://doi.org/10.1016/j.jbiomech.2013.06.022

RunScribe. (n.d.) RunScribe Metrics. Retrieved January 9, 2023, from https://runscribe.com/metrics/

Sasimontonkul, S., Bay, B. K., & Pavol, M. J. (2007). Bone contact forces on the distal tibia during the stance phase of running. *Journal of Biomechanics*, *40*(15), 3503–3509. https://doi.org/10.1016/j.jbiomech.2007.05.024

Saunier, J., & Chapurlat, R. (2018). Stress fracture in athletes. *Joint, Bone, Spine*, *85*(3), 307–310. https://doi.org/10.1016/j.jbspin.2017.04.013

Scott, S. H., & David, A. W. (1990). Internal forces at chronic running injury sites. *Medical Science*, *22*(3), 357–369. https://doi.org/10.1249/00005768-199006000-00013

Sheerin, K. R., Reid, D., & Besier, T. F. (2019). The measurement of tibial acceleration in runners—A review of the factors that can affect tibial acceleration during running and evidence-based guidelines for its use. *Gait & Posture*, *67*(September 2018), 12–24. https://doi.org/10.1016/j.gaitpost.2018.09.017

Sinclair, J. (2014). Effects of barefoot and barefoot inspired footwear on knee and ankle loading during running. *Clinical Biomechanics*, *29*(4), 395–399. https://doi.org/10.1016/j.clinbiomech.2014.02.004

Taunton, J. E., Ryan, M. B., Clement, D. B., McKenzie, D. C., Lloyd-Smit, D. R., & Zumbo, D. B. (2002). A retrospective case-control analysis of 2002 running injuries. *British Journal of Sports Medicine*, *36*, 95–101. https://doi.org/10.1136/bjsm.36.2.95

Umans, H., & Pavlov, H. (1994). Stress fractures of the lower extremities. *Seminars in Roentgenology*, *29*(2), 176–193. https://doi.org/10.1016/S0037-198X(05)80063-X

Van den Berghe, P., Six, J., Gerlo, J., Leman, M., & De Clercq, D. (2019). Validity and reliability of peak tibial accelerations as real-time measure of impact loading during over-ground rearfoot running at different speeds. *Journal of Biomechanics*, *86*, 238–242. https://doi.org/10.1016/j.jbiomech.2019.01.039

Wall, J., & Feller, J. F. (2006). Imaging of stress fractures in runners. *Clinics in Sports Medicine*, *25*(4), 781–802. https://doi.org/10.1016/j.csm.2006.06.003

Willy, R. W., Halsey, L., Hayek, A., & Willson, J. D. (2016). Overground and treadmill comparison of patellofemoral joint and achilles tendon loads. *Journal of Orthopaedic & Sports Physical Therapy*, *46*(8), 1–31. https://www.jospt.org/doi/10.2519/jospt.2016.6494

Xsens Technologies B.V. (2021). MVN user manual. *MVN Man,* (April), 162. https://www.cleancss.com/user-manuals/QIL/MTW2-3A7G6

Zadpoor, A. A., & Nikooyan, A. A. (2011). The relationship between lower-extremity stress fractures and the ground reaction force: A systematic review. *Clinical Biomechanics*, *26*(1), 23–28. https://doi.org/10.1016/j.clinbiomech.2010.08.005

Zifchock, R. A., Davis, I., Higginson, J., McCaw, S., & Royer, T. (2008). Side-to-side differences in overuse running injury susceptibility: A retrospective study. *Human Movement Science*, *27*(6), 888–902. https://doi.org/10.1016/j.humov.2008.03.007

Appendix

This appendix describes the analysis of an online dataset (Matijevich et al., 2019) to develop and validate a method to spatially align IMU-derived data expressed in a global IMU-based coordinate system $\Psi^{gl,imu}$, with force plate data expressed in a global force plate-based coordinate system $\Psi^{gl,fp}$.

Force plate and optical motion analysis data of 10 runners running at eight different speeds (ranging from 9.4 to 14.4 km/h) on a level treadmill were extracted from an online dataset (Matijevich et al., 2019). More details about the study protocol can be found in the original article accompanying the online dataset (Matijevich et al., 2019).

The stance phase of running was defined as the period where the vertical GRF was larger than 20 N (Milner & Paquette, 2015). The stance phase started with initial contact and ended with toe-off. To be representative of the population used in the main study, only rearfoot striking runners were included. A rearfoot strike was defined as a mean foot contact angle at initial contact of 8 degrees or more (Altman & Davis, 2012). The mean foot contact angle was defined as the sagittal plane angle between a line from the right heel to the right toe marker and the horizontal at initial contact (Altman & Davis, 2012). Four out of 10 runners had a foot contact angle smaller than 8 degrees and were classified as non-rearfoot strikers and excluded from further analysis.

Ground reaction forces (GRF) and ground reaction moments (GRM) were filtered with a third-order recursive Butterworth filter of 15 Hz (Matijevich et al., 2019). The centre of pressure (COP) in the running direction (COP_x) was computed:

$$COP_x = \frac{GRM_z}{GRF_y} \tag{4}$$

where GRM_z represents GRM around the Z-axis (sidewards) of $\Psi^{gl,fp}$ and where GRF_y represents the vertical GRF in $\Psi^{gl,fp}$.

Positions of the right heel, right toe, and fifth metatarsal marker (MT5) were extracted and filtered with a third-order recursive Butterworth filter of 10 Hz (Matijevich et al., 2019). In one subject, the right toe marker was not present; in this case, the position of the right first metatarsal marker (MT1) was extracted and filtered instead of MT5 to compute the foot contact angle.

The first 24 strides for each speed of all included subjects were used for analysis since each trial consisted of at least 24 strides. COP_x and the forward position of the MT5 marker ($MT5_x$) were normalised to the percentage of the stance phases. The percentage of the stance phase at which COP_x crossed $MT5_x$ was computed and averaged for all steps. On average, COP_x crossed $MT5_x$ at 62 ± 12% of the stance phase, see Table 2.

To quantify the error introduced by assuming that COP_x crossed $MT5_x$ at 62% of the stance phase in all rearfoot striking runners, the positional difference between COP_x and $MT5_x$ for all subjects, and speeds at 62% of the stance phase were computed. This error was, on average 12 ± 15 mm, see Table 2.